molecular pharmaceutics

articles

Ultrasound Exposure of Lipoplex Loaded Microbubbles Facilitates Direct Cytoplasmic Entry of the Lipoplexes

Ine Lentacker,[†,‡] Nan Wang,[†] Roosmarijn E. Vandenbroucke,[†] Jo Demeester,[†] Stefaan C. De Smedt,*[,†] and Niek N. Sanders[§]

Laboratory of General Biochemistry and Physical Pharmacy, Ghent Research Group on Nanomedicine, Faculty of Pharmaceutical Sciences, Ghent University, Harelbekestraat 72, B-9000 Ghent, Belgium, and Laboratory of Gene Therapy, Department of Nutrition, Genetics and Ethology, Faculty of Veterinary Medicine, Ghent University, Heidestraat 19, B-9820 Merelbeke, Belgium

Received September 8, 2008; Revised Manuscript Received December 3, 2008; Accepted December 30, 2008

Abstract: Recently we reported that the transfection of cells by PEGylated lipoplexes becomes significantly better by binding the PEGylated lipoplexes to the surface of microbubbles and applying ultrasound. To further optimize this gene delivery system it is important to understand the working mechanism. This paper elucidates the cellular entry path of these lipoplexes. The results clearly show that the PEGylated lipoplexes, released from the microbubbles upon applying ultrasound, are not taken up by endocytosis, the most common route for nanoparticles to enter cells. Our data demonstrate that, upon implosion of the microbubbles, the PEGylated lipoplexes are released and are most probably able to passively diffuse through the cell membrane pores or become injected in the cytoplasm of the target cells. This is attractive as the *in vivo* use of PEGylated nanoparticles remains currently limited due to a decreased cellular uptake and inefficient escape of the PEGylated nanoparticles from the endosomes.

Keywords: Ultrasound; microbubbles; intracellular pathway; PEGylated lipoplexes; microjets

Introduction

The development of safe and efficient gene delivery systems is crucial for *in vivo* gene therapy. Viral delivery systems are the most efficient gene delivery systems. However, their *in vivo* use has been limited after the death of several patients during clinical trials with both adenoviral and adenoassociated viral (AAV) vectors.[1] Furthermore, viral delivery systems are expensive while, especially, AAV vectors cannot host (very) large transgenes. Also the risk of insertional mutagenesis and severe immune responses limit their *in vivo* use. In contrast, nonviral gene delivery systems have several advantages: easy and cheap production and the possibility of incorporating large plasmids.[2] Furthermore they cause a relatively lower immune response.[2] To improve the efficiency of nonviral delivery systems researchers have upgraded them with different functionalities like targeting ligands and fusiogenic peptides to enable their endosomal escape. The latter is important as almost all nonviral vectors are taken up via endocytosis. Additionally, to avoid (a) aggregation in blood and (b) interaction with blood compounds like albumin, the surface of many types of nonviral delivery systems has been covered with polymers like poly

* Corresponding author. Mailing address: Laboratory of General Biochemistry and Physical Pharmacy, Ghent Research Group on Nanomedicine, Faculty of Pharmaceutical Sciences, Ghent University, Harelbekestraat 72, B-9000 Ghent, Belgium. E-mail: Stefaan.DeSmedt@UGent.be. Tel: +32 (09) 264 80 76. Fax: +32 (09) 264 81 89.

[†] Laboratory of General Biochemistry and Physical Pharmacy, Ghent Research Group on Nanomedicine, Faculty of Pharmaceutical Sciences.

[‡] E-mail: Ine.Lentacker@UGent.be.

[§] Laboratory of Gene Therapy, Department of Nutrition, Genetics and Ethology, Faculty of Veterinary Medicine.

(1) Marshall, E. Gene Therapy Death Prompts Review of Adenovirus Vector. *Science* **1999**, 2244–2245.

(2) Patil, S. D.; Rhodes, D. G.; Burgess, D. J. DNA-based therapeutics and DNA delivery systems: a comprehensive review. *AAPS J.* **2005**, *7* (1), E61−E77.

10.1021/mp800154s CCC: $40.75
Published on Web 01/30/2009

ethylene-glycol (PEG).[3−5] However, PEGylation drastically lowers the transfection efficiency of nonviral vectors by hampering their cellular uptake and endosomal release. Therefore, PEG chains have been attached to lipids and polymers via chemical bonds that become cleaved in the acidic environment of the late endosomes. However, the synthesis of such so-called "bioresponsive" carriers remains rather difficult.[6,7]

Recently, the use of ultrasound and microbubbles has gained more and more attention to deliver drugs, especially nucleic acids.[8] Although microbubbles are currently used as contrast agent in ultrasound imaging,[9] they can also provoke several cellular effects. At low ultrasound intensities, the microbubbles oscillate linearly in the acoustic pressure waves, a phenomenenon called stable cavitation. This results in microstreaming, which affects the cellular membrane when the microbubbles are located close enough to the cells.[10] At higher ultrasound intensities, the expansions of the microbubbles become larger followed by a violent collapse of the microbubbles that results in shock waves that can temporarily perforate cell membranes (this phenomenon is called sonoporation). This collapse is due to the inertia of the inrushing fluid and is therefore called inertial cavitation.[11] Ultrasound assisted drug delivery has many advantages, and one of the most attractive properties is the potential for time and space controlled delivery of drugs. On top, microbubbles and ultrasound energy are considered relatively safe as both have been applied in medical imaging for several years.[12]

Ultrasound in combination with microbubbles has been intensively evaluated to enhance the delivery of *naked* DNA (genes and antisense oligonucleotides) and siRNA.[13−21] However, to obtain a significantly higher biological effect large amounts of DNA and siRNA are required. This is due to the fact that naked DNA and siRNA are sensitive to degradation by nucleases, which are widely distributed in the body. Also, as the ultrasound induced pores in the cell membranes are short lived, large amounts of DNA and siRNA are required near the pores to ensure a sufficient influx inside the cells.

To overcome the limitations of (a) naked DNA combined with ultrasound and microbubbles and (b) PEGylated lipoplexes (which suffer from an inefficient cellular uptake and endosomal escape), we previously coupled PEGylated lipoplexes onto ultrasound responsive microbubbles (Figure 1),[22,23] the idea being that the lipoplexes will be released upon ultrasound treatment and that they will be more easily transported inside the cell. Applying ultrasound to PEGylated lipoplexes bound to microbubbles resulted in much higher transfection when compared to the transfection obtained with free PEGylated lipoplexes with or without the use of microbubbles and ultrasound (Figure 2B). To further optimize this new delivery system it is necessary to understand

(3) Eliyahu, H.; Servel, N.; Domb, A. J.; Barenholz, Y. Lipoplex-induced hemagglutination: potential involvement in intravenous gene delivery. *Gene Ther.* **2002**, *9* (13), 850–858.
(4) Sakurai, F.; Nishioka, T.; Yamashita, F.; Takakura, Y.; Hashida, M. Effects of erythrocytes and serum proteins on lung accumulation of lipoplexes containing cholesterol or DOPE as a helper lipid in the single-pass rat lung perfusion system. *Eur. J. Pharm. Biopharm.* **2001**, *52* (2), 165–172.
(5) Moghimi, S. M.; Szebeni, J. Stealth liposomes and long circulating nanoparticles: critical issues in pharmacokinetics, opsonization and protein-binding properties. *Prog. Lipid Res.* **2003**, *42* (6), 463–478.
(6) Meyer, M.; Wagner, E. Recent developments in the application of plasmid DNA-based vectors and small interfering RNA therapeutics for cancer. *Hum. Gene Ther.* **2006**, *17* (11), 1062–1076.
(7) Wong, J. B.; Grosse, S.; Tabor, A. B.; Hart, S. L.; Hailes, H. C. Acid cleavable PEG-lipids for applications in a ternary gene delivery vector. *Mol. Biosyst.* **2008**, *4* (6), 532–541.
(8) Hernot, S.; Klibanov, A. L. Microbubbles in ultrasound-triggered drug and gene delivery. *Adv. Drug Delivery Rev.* **2008**, *60* (10), 1153–1166.
(9) Riess, J. G. Fluorocarbon-based injectable gaseous microbubbles for diagnosis and therapy. *Curr. Opin. Colloid Interface Sci.* **2003**, *8* (3), 259–266.
(10) Ohl, C.-D.; Arora, M.; Ikink, R.; de Jong, N.; Versluis, M.; Delius, M.; Lohse, D. Sonoporation from jetting cavitation bubbles. *Biophys. J.* **2006**, *91* (11), 4285–4295.
(11) Newman, C. M. H.; Bettinger, T. Gene therapy progress and prospects: Ultrasound for gene transfer. *Gene Ther.* **2007**, *14* (6), 465–475.
(12) Grayburn, P. A. Current and future contrast agents. *Echocardiography* **2002**, *19* (3), 259–265.
(13) Bekeredjian, R.; Chen, S. Y.; Grayburn, P. A.; Shohet, R. V. Augmentation of cardiac protein delivery using ultrasound targeted microbubble destruction. *Ultrasound Med. Biol.* **2005**, *31* (5), 687–691.
(14) Duvshani-Eshet, M.; Machluf, M. Therapeutic ultrasound optimization for gene delivery: A key factor achieving nuclear DNA localization. *J. Controlled Release* **2005**, *108* (2−3), 513–528.
(15) Kinoshita, M.; Hynynen, K. A novel method for the intracellular delivery of siRNA using microbubble-enhanced focused ultrasound. *Biomed. Biophys. Res. Commun.* **2005**, *335* (2), 393–399.
(16) Kinoshita, M.; Hynynen, K. Intracellular delivery of Bak BH3 peptide by microbubble-enhanced ultrasound. *Pharm. Res.* **2005**, *22* (5), 716–720.
(17) Manome, Y.; Nakayama, N.; Nakayama, K.; Furuhata, H. Insonation facilitates plasmid DNA transfection into the central nervous system and microbubbles enhance the effect. *Ultrasound Med. Biol.* **2005**, *31* (5), 693–702.
(18) Mehier-Humbert, S.; Bettinger, T.; Yan, F.; Guy, R. H. Plasma membrane poration induced by ultrasound exposure: Implication for drug delivery. *J. Controlled Release* **2005**, *104* (1), 213–222.
(19) Newman, C. M.; Lawrie, A.; Brisken, A. F.; Cumberland, D. C. Ultrasound gene therapy: On the road from concept to reality. *Echocardiography* **2001**, *18* (4), 339–347.
(20) Pislaru, S. V.; Pislaru, C.; Kinnick, R. R.; Singh, R.; Gulati, R.; Greenleaf, J. F.; Simari, R. D. Optimization of ultrasound-mediated gene transfer: comparison of contrast agents and ultrasound modalities. *Eur. Heart J.* **2003**, *24* (18), 1690–1698.
(21) Vannan, M.; McCreery, T.; Li, P.; Han, Z. G.; Unger, E.; Kuersten, B.; Nabel, E.; Rajagopalan, S. Ultrasound-mediated transfection of canine myocardium by intravenous administration of cationic microbubble-linked plasmid DNA. *J. Am. Soc. Echocardiogr.* **2002**, *15* (3), 214–218.

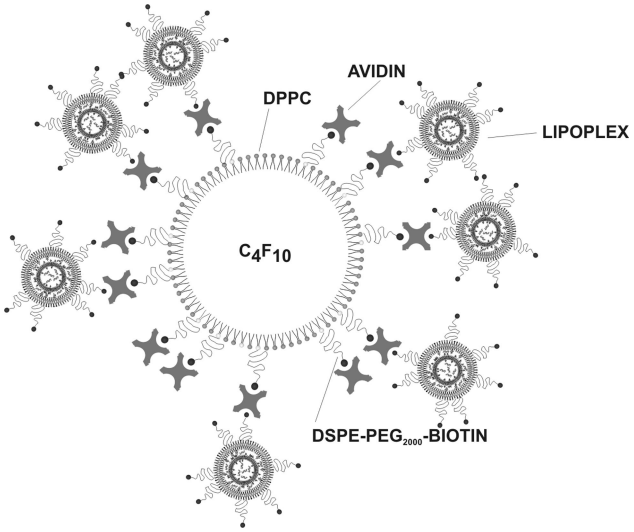

Figure 1. Schematic presentation of lipoplex loaded microbubbles.

the mechanism which explains this higher transfection efficiency. Therefore, the aim of this work was to elucidate the cellular pathway by which PEGylated lipoplexes, upon release from the microbubbles by ultrasound, enter the cells.

Materials and Methods

Preparation and Characterization of Lipid Microbubbles Containing DSPE-PEG-Biotin. Liposomes containing DPPC (dipalmitoylphosphatidylcholine) and DSPE-PEG-biotin (1,2-distearoyl-*sn*-glycero-3-phosphoethanolamine-*N*-(biotinyl(polyethyleneglycol)2000)) in a 95:5 molar ratio were prepared as previously described.[24] Briefly, the lipids were put in a round-bottomed flask, dissolved in chloroform. Subsequently, the solvent was removed via evaporation followed by flushing with nitrogen. The obtained lipid film was hydrated in HEPES buffer (20 mM HEPES, pH 7.4) at a final lipid concentration of 5 mg/mL and incubated overnight at 4 °C to allow the formation of liposomes. The resulting liposomes were first extruded through a polycarbonate membrane (pore size of 0.2 μm) using a miniextruder (Avanti Polar Lipids, Alabaster, AL). Subsequently, the extruded liposomes were sonicated with a 20 kHz probe (Branson 250 sonifier, Branson Ultrasonics Corp., Danbury, CT) in the presence of perfluorobutane gas (C_4F_{10}, MW 238 g/mol, F2 chemicals, Preston, Lancashire, U.K.). After sonication the microbubbles were washed (to remove the excess of lipids) with 3 mL of fresh HEPES buffer and finally resuspended in 5 mL. To enable the attachment of biotinylated lipoplexes, the biotinylated microbubbles were incubated with 500 μL of avidin (10 mg/mL) and incubated for 10 min at room temperature. Subsequently, the microbubbbles were centrifuged and washed again with 3 mL of fresh HEPES buffer. Finally the microbubbles were resuspended in 5 mL of HEPES buffer. The concentration of the avidinylated microbubbles in the dispersions was determined with the aid of a Burker chamber and a light microscope and equaled 4×10^8 microbubbles/mL.

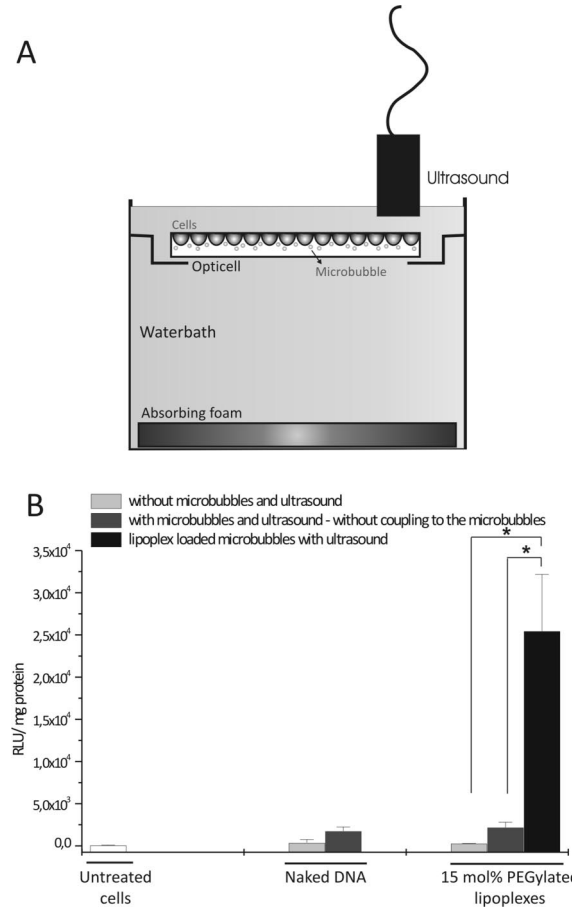

Figure 2. (A) Schematic representation of the experimental setup. Cells were grown on one side of an Opticell unit. For ultrasound exposure, Opticell plates were turned upside down. In this way, microbubbles were able to rise against the cell layer. (B) The transfection efficiency of lipoplex loaded microbubbles in the presence of ultrasound (black bars) compared to the transfection efficiency of naked DNA and free 15 mol % PEGylated lipoplexes in the absence (light gray bars) and presence of microbubbles and ultrasound (dark gray bars). The background luciferase signal in untreated cells is also shown (white bars). The transfection results, i.e., the extent of luciferase expression, are expressed as RLU (RLU: relative light units) per mg protein. *$p < 0.05$.

Preparation and Characterization of PEGylated Cationic Liposomes and Lipoplexes. The cationic lipid DOTAP (*N*-(1-(2,3-dioleoyloxy)propyl)-*N*,*N*,*N*-trimethylammonium

(22) Lentacker, I.; De Geest, B. G.; Vandenbroucke, R. E.; Peeters, L.; Demeester, J.; De Smedt, S. C.; Sanders, N. N. Ultrasound-responsive polymer-coated microbubbles that bind and protect DNA. *Langmuir* **2006**, *22* (17), 7273–7278.

(23) Vandenbroucke, R. E.; Lentacker, I.; Demeester, J.; De Smedt, S. C.; Sanders, N. N. Ultrasound assisted siRNA delivery using PEG-siPlex loaded microbubbles. *J. Controlled Release* **2008**, *126* (3), 265–273.

(24) Sanders, N. N.; Van Rompaey, E.; De Smedt, S. C.; Demeester, J. Structural alterations of gene complexes by cystic fibrosis sputum. *Am. J. Respir. Crit. Care Med.* **2001**, *164* (3), 486–493.

chloride), the phospholipid DOPE (dioleoyl phosphatidyl ethanolamine), DSPE-PEG, DSPE-PEG-biotin and cholesteryl Bodipy FLC12 (cholesteryl 4,4-difluoro-5,7-dimethyl-4-bora-3a,4a-diaza-*s*-indacene-3-dodecanoate) were purchased from Avanti Polar Lipids. Cationic liposomes containing DOTAP and DOPE in a 1:1 molar ratio with 0 to 15 mol % DSPE-PEG or DSPE-PEG-biotin were prepared as described above.

For the preparation of lipoplexes we used plasmid DNA (pDNA; pGL3, Promega, Leiden, The Netherlands) containing the luciferase gene from *Photinus pyralis* as reporter (i.e., firefly luciferase). The pDNA was amplified in *Escherichia coli* and purified as described elsewhere.[24] The pDNA was dissolved in HEPES buffer, and the concentration was set at 1.0 mg/mL, taking into account that the absorption at 260 nm of a 50 μg/mL DNA solution equals 1. The pDNA showed a high purity as the ratio of the absorption at respectively 260 and 280 nm was between 1.8 and 2.0.

Lipoplexes were prepared at a charge ratio of 4. The charge ratio is defined as the ratio of the number of the positive charges (originating from DOTAP) to the number of the negative charges (originating from the pDNA). pDNA was first diluted in HEPES buffer to a concentration of 0.41 mg/mL. Subsequently, the diluted pDNA was added to an equal volume of cationic liposomes (5 mM DOTAP) resulting in a final $\pm$ charge ratio of 4. Immediately after the addition of pDNA to the cationic liposomes, HEPES buffer was added until the final concentration of pDNA in the system was 0.126 mg/mL. This mixture was then vortexed and incubated at room temperature for 30 min. To fluorescently label the liposomes 0.5 mol % cholesteryl Bodipy FLC12 (cholesteryl 4,4-difluoro-5,7-dimethyl-4-bora-3a,4a-diaza-*s*-indacene-3-dodecanoate) was used (Molecular probes, Eugene OR).

Melanoma Cells Stably Expressing Renilla Luciferase (rLuc). BLM_rLuc cells stably expressing renilla luciferase were generated by transfecting BLM-cells (melanoma cells)[25] with the pGL4.76_CMV plasmid. The pGL4.76_CMV plasmid was generated by ligating the PCR amplified (forward primer AATAGTCGACTAGTTATTAATAGTAATCAA and reversed primer AATAGGATCCGATCTGACGGTTCACTAAAC) and *Sal*I/*Bam*HI double digested CMV promotor into the *Xho*I/*Bgl*II double digested pGL4.76 plasmid (Promega, Leiden, The Netherlands). The resulting pGL4.76_CMV plasmid was linearized with the *Bam*HI restriction enzyme and complexed with linear polyethylenimine (PEI; 22 kDa) to transfect the BLM cells. Transfected cells were incubated in fresh medium for 48 h and then selected with 250 μg/mL hygromycin. After two weeks, clones were isolated and expanded. Subsequently, the generated clones were analyzed and a renilla luciferase positive clone was selected.

Transfection Experiments. BLM-cells were cultured in Dulbecco's modified Eagle's medium (DMEM) with the growth factor F12 and phenol red containing 2 mM glutamine, 10% heat deactivated fetal bovine serum (FBS), 1% penicillin-streptomycin (Gibco, Merelbeke, Belgium) and HEPES buffer (100 mM, pH 7.4). Cells were grown to 90% confluency in OptiCell units (Biocrystal, Westerville, OH) in a humidified incubator at 37 °C and 5% CO_2. Subsequently, cells were washed with 10 mL of phosphate buffered saline (PBS, Gibco) and the transfection medium was added.

A first transfection medium was prepared by mixing 130 μL of PEGylated lipoplexes with 1 mL of the microbubble suspension (containing 4×10^8 microbubbles). After 5 min of incubation at room temperature, OPTIMEM (Gibco, Merelbeke, Belgium) was added to a final volume of 10 mL. A second transfection medium was prepared in a similar way except that the 130 μL of PEGylated lipoplexes was replaced by an equal volume of HEPES buffer containing 16.5 μg of pDNA, the same amount as present in the lipoplexes.

The 10 mL of transfection medium was completely added to the OptiCell units (surface 50 cm^2). Subsequently, the cells were placed in a water bath at 37 °C with an absorbing rubber at the bottom and immediately subjected to ultrasound radiation. The ultrasound radiation was performed for 10 s with a sonitron 2000 (RichMar, Inola, OK) equipped with a 22 mm probe. A schematic representation of the experimental setup used is displayed in Figure 2A. In all ultrasound experiments the following ultrasound settings were applied: 1 MHz, 10% duty cycle and an ultrasound intensity of 2 W/cm^2. The areas treated with ultrasound were marked, and after radiation, the OptiCells were incubated for an additional 2 h at 37 °C. At the end of this incubation period, the transfection medium was removed and the cells were washed two times with PBS, before adding fresh culture medium. Each transfection was performed in 3-fold. Twenty-four hours after transfection the firefly luciferase expression by the cells was analyzed. Therefore, the culture medium was removed and cells were washed with PBS. The areas exposed to ultrasound (20 mm diameter) were cut from the opticell membrane and brought into a 24-well plate. Eighty microliters of CCLR (Cell Culture Lyse Reagent, Promega, Leiden, The Netherlands) buffer was added to each well and incubated at room temperature for at least 20 min to allow cell lysis. Twenty microliteres of the cell lysate was transferred to a 96-well plate and the luciferase activity was measured using the Glomax 96 Microplate Luminometer (Promega) as described elsewhere.[26] An aliquot (20 μL) of each cell lysate was also analyzed for protein concentration using the BCA protein Assay (Pierce, Rockford, IL). Transfection results are expressed as relative light units (RLU) per mg protein.

In the transfection experiment with methyl-β-cyclodextrin (MβCD), the BLM cell line stably expressing renilla lu-

(25) Quax, P. H. A.; Vanmuijen, G. N. P.; Weeningverhoeff, E. J. D.; Lund, L. R.; Dano, K.; Ruiter, D. J.; Verheijen, J. H. Metastatic Behavior of Human-Melanoma Cell-Lines in Nude-Mice Correlates with Urokinase-Type Plasminogen-Activator, Its Type-1 Inhibitor, and Urokinase-Mediated Matrix Degradation. *J. Cell Biol.* **1991**, *115* (1), 191–199.

(26) von Gersdorff, K.; Sanders, N. N.; Vandenbroucke, R.; De Smedt, S. C.; Wagner, E.; Ogris, M. The internalization route resulting in successful gene expression depends on polyethylenimine both cell line and polyplex type. *Mol. Ther.* **2006**, *14* (5), 745–753.

ciferase (BLM_rLuc) was used. The cells were preincubated for two hours with MβCD before the addition of the lipoplexes or lipoplex loaded microbubbles. Ultrasound radiation was carried out as described above. Both, firefly and renilla luciferase were measured with the Dual-Luciferase Reporter Assay System (Promega, Leiden, The Netherlands) in the Glomax 96 Microplate Luminometer (Promega). Results were expressed as firefly RLU/renilla RLU.

Photochemical Internalization Experiments. The photosensitizer (PS) TPPS2a, meso-tetraphenylporphine with two sulfonate groups on adjacent phenyl rings, was kindly provided by Dr. Anders Høgset (PCI Biotech AS, Oslo, Norway). The PS was light protected and stored at 4 °C until use. Cells were exposed to blue light from the LumiSource, a bank of four light tubes emitting light in the region of 375−450 nm, with 13 mW/cm^2 irradiance (PCI Biotech AS, Oslo, Norway). Cells were incubated overnight with 0.8 μg/mL PS. The day after, the PS was removed and cells were incubated with lipoplexes or transfected with lipoplex loaded microbubbles and exposed to ultrasound. After 2 h incubation time, the transfection medium was removed and cells were incubated at 37 °C for an additional 2 h with culture medium. Subsequenly the cells were exposed to the Lumisource for 40s and again placed at 37 °C. Cells were analyzed 24 h later.

Confocal Experiments. BLM-cells were seeded into culture dishes or opticell plates one day before the confocal experiment. The cell membrane was labeled with concanavalin A-Alexa647 (Molecular Probes). The concanavalin A stock solution was diluted 10-fold in OPTIMEM and added to the cells immediately before visualization. Cells were incubated with the free PEGylated lipoplexes for respectively 30 and 150 min at 37 °C and 5% CO_2. Ultrasound exposure of BLM-cells was performed immediately after addition of the lipoplex loaded microbubbles and cells were incubated then at 37 °C for respectively 30 and 150 min. After the incubation time, cells were visualized using a Nikon EZC1-si confocal laser scanning microscope (Nikon, Brussels, Belgium) equipped with a 40× objective. The 491 nm line of this microscope was used to excite the Bodipy label. The 639 nm line was used to excite concanavalin A-Alexa647.

Propidium Iodide (PI) Uptake. PI was added to the cells in a concentration of 25 μg/mL in OPTIMEM. The PI was added either before the exposure of the cells to lipoplex loaded microbubbles and ultrasound or afterward. The uptake of PI resulted in the appearance of red fluorescent nuclei, that were visualized with the 639 nm laser of the Nikon EZC1-si confocal microscope.

Statistical Analysis. All the data in this report are expressed as mean ± standard deviation (SD). For the transfection results, Student's *t* test was used to determine whether data groups differed significantly from each other. A *p*-value lower than 0.05 was considered statistically significant.

Results and Discussion

Design and Transfection Efficiency of Lipoplex Loaded Microbubbles. As schematically presented in Figure 1, we earlier succeeded in coupling highly PEGylated lipoplexes onto lipid microbubbles with the aid of an avidin−biotin link.[22] Biotinylated lipid microbubbles consisting of DPPC and DSPE-PEG-biotin were prepared next to DOTAP/DOPE based lipoplexes with 15 mol % DSPE-PEG-biotin. Subsequently, avidin was bound to the biotinylated microbubbles and mixed with the biotinylated lipoplexes. As published previously,[22] exposure of these lipoplex loaded microbubbles to ultrasound caused a massive release of intact lipoplexes and drastically increased the transfection efficiency of the PEGylated lipoplexes. Figure 2B shows the transfection of cells by respectively free PEGylated lipoplexes (light gray bars), PEGylated lipoplexes physically mixed with microbubbles (dark gray bars) and lipoplex loaded microbubbles after exposure to ultrasound (black bars). Only the PEGylated lipoplexes that were coupled to the microbubbles were able to transfect the cells after ultrasound radiation (black bars). It has been postulated that sonication of free lipoplexes could increase their transfection efficiency, but this was not confirmed in our experiments[27−29] in agreement with the observations by Mehier-Humbert and colleagues.[18] Considering the giant increase in transfection efficiency after coupling the PEGylated lipoplexes to the microbubbles, we wanted to elucidate the differences in cellular uptake between respectively "free" PEGylated lipoplexes and PEGylated lipoplexes released from the lipoplex loaded microbubbles by ultrasound.

Which Mechanism Do Lipoplexes Use To Enter Cells after Exposure of Lipoplex Loaded Microbubbles to Ultrasound? (a) Influence of the Endocytic Inhibitor Methyl-β-cyclodextrin (MβCD). The intracellular uptake of lipoplexes has been intensively studied and has been ascribed to endocytosis.[30] It is believed that the main reasons for the low transfection efficiency of highly PEGylated lipoplexes are their limited endocytic uptake (as the PEG chains prevent association of the lipoplexes with the cellular membrane) and, especially, their difficulties to escape from

(27) Unger, E. C.; McCreery, T. P.; Sweitzer, R. H. Ultrasound enhances gene expression of liposomal transfection. *Invest. Radiol.* **1997**, *32* (12), 723–727.

(28) Koch, S.; Pohl, P.; Cobet, U.; Rainov, N. G. Ultrasound enhancement of liposome-mediated cell transfection is caused by cavitation effects. *Ultrasound Med. Biol.* **2000**, *26* (5), 897–903.

(29) Lawrie, A.; Brisken, A. F.; Francis, S. E.; Cumberland, D. C.; Crossman, D. C.; Newman, C. M. Microbubble-enhanced ultrasound for vascular gene delivery. *Gene Ther.* **2000**, *7* (23), 2023–2027.

(30) Wasungu, L.; Hoekstra, D. Cationic lipids, lipoplexes and intracellular delivery of genes. *J. Controlled Release* **2006**, *116* (2), 255–264.

the endosomes.[31−35] As lipoplex loaded microbubbles are able to transfect BLM cells efficiently after ultrasound exposure (Figure 2B), we hypothesize that the PEGylated lipoplexes released from microbubbles by ultrasound do not enter the cell through an endocytic pathway. To evaluate this hypothesis, we first investigated the effect of inhibitors on the cellular uptake and transfection efficiency of respectively free lipoplexes and lipoplex loaded microbubbles exposed to ultrasound. We tested the effect of different endocytosis-interfering drugs (chlorpromazin, filipin, genistein, methyl-β-cyclodextrin, nystatin) on the transfection efficiency of free DOTAP/DOPE lipoplexes without or with 5 mol % DSPE-PEG. The 15 mol % PEGylated lipoplexes were excluded in this experiment, as the transfection efficiency of these lipoplexes (in the absence of microbubbles and ultrasound) is too low to observe any influence of an endocytic inhibitor. We found that MβCD, which depletes cholesterol from the cell membrane, caused the strongest inhibition of the gene expression of these lipoplexes (data not shown). This suggests a cholesterol-dependent uptake pathway in the BLM cells for the free DOTAP/DOPE lipoplexes. This is in agreement with the work of Zuhorn et al.[36] who showed that cholesterol depletion of cells can extensively decrease the internalization of SAINT-2/DOPE lipoplexes. To ensure that the decrease in gene expression caused by MβCD is really due to reduced endosomal uptake and not due to toxic effects on the cells, we evaluated the cytotoxicity of MβCD. As depicted in Figure 3, MβCD was not toxic for the BLM cells up to a concentration of 1500 μM, i.e. the highest concentration used in our experiments.

Subsequently we studied the effect of MβCD on the transfection efficiency of (a) non-PEGylated lipoplexes, (b) 5 mol % PEGylated lipoplexes and (c) microbubbles loaded with PEGylated lipoplexes exposed to ultrasound. As demonstrated in Figure 4, even the lowest MβCD concentrations had an influence on the transfection efficiency of the non-

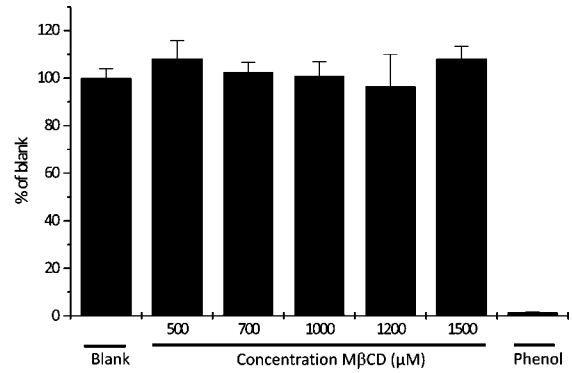

Figure 3. Cell viability of the BLM cells after incubation with different MβCD concentrations. Results are expressed as a percentage of the viability of untreated cells (blank). Phenol (10 mg/mL) was used as a positive control.

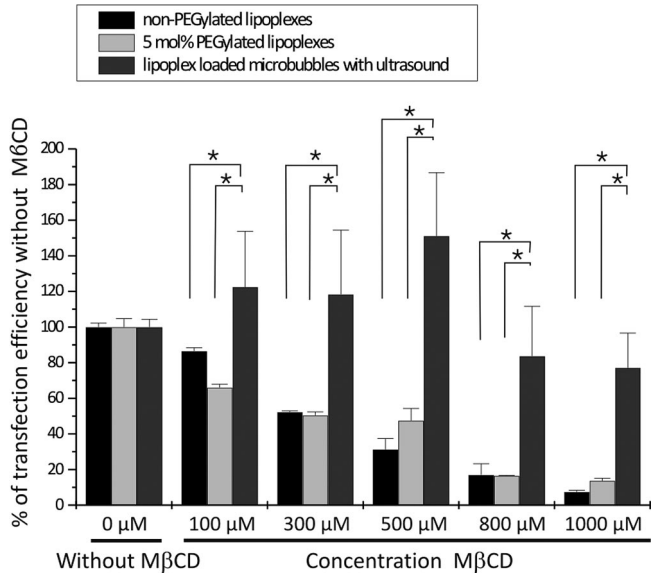

Figure 4. Effect of increasing MβCD concentrations on the transfection efficiency of non-PEGylated (black bars), 5 mol % PEGylated lipoplexes (light gray bars) and lipoplex loaded microbubbles (dark gray bars) exposed to ultrasound. Results are expressed as a percentage of the transfection efficiency obtained in cells in the absence of MβCD. *$p < 0.05$.

PEGylated (black bars) and PEGylated lipoplexes (light gray bars). Increasing the concentration of MβCD clearly diminished their transfection efficiency further. Via confocal microscopy we confirmed that MβCD reduced the gene expression of the lipoplexes by lowering the cellular uptake of the lipoplexes. Figure 5A,B shows the uptake of the non-PEGylated lipoplexes by BLM cells in the absence of MβCD. A major part of the lipoplexes can be detected in the intracellular space. Incubation of the cells with 500 μM MβCD (Figure 5C,D), and especially 1000 μM MβCD (Figure 5E,F), almost completely blocked the cellular uptake of non-PEGylated lipoplexes. Similar images were obtained with the PEGylated lipoplexes (data not shown).

(31) Song, L. Y.; Ahkong, Q. F.; Rong, Q.; Wang, Z.; Ansell, S.; Hope, M. J.; Mui, B. Characterization of the inhibitory effect of PEG-lipid conjugates on the intracellular delivery of plasmid and antisense DNA mediated by cationic lipid liposomes. *Biochim. Biophys. Acta* **2002**, *1558* (1), 1–13.

(32) Shi, F. X.; Wasungu, L.; Nomden, A.; Stuart, M. C. A.; Polushkin, E.; Engberts, J. B. F. N.; Hoekstra, D. Interference of poly(ethylene glycol)-lipid analogues with cationic-lipid-mediated delivery of oligonucleotides; role of lipid exchangeability and non-lamellar transitions. *Biochem. J.* **2002**, *366*, 333–341.

(33) Mishra, S.; Webster, P.; Davis, M. E. PEGylation significantly affects cellular uptake and intracellular trafficking of non-viral gene delivery particles. *Eur. J. Cell Biol.* **2004**, *83* (3), 97–111.

(34) Meyer, O.; Kirpotin, D.; Hong, K. L.; Sternberg, B.; Park, J. W.; Woodle, M. C.; Papahadjopoulos, D. Cationic liposomes coated with polyethylene glycol as carriers for oligonucleotides. *J. Biol. Chem.* **1998**, *273* (25), 15621–15627.

(35) Audouy, S.; Hoekstra, D. Cationic lipid-mediated transfection in vitro and in vivo. *Mol. Membr. Biol.* **2001**, *18* (2), 129–143.

(36) Zuhorn, I. S.; Kalicharan, R.; Hoekstra, D. Lipoplex-mediated transfection of mammalian cells occurs through the cholesterol-dependent clathrin-mediated pathway of endocytosis. *J. Biol. Chem.* **2002**, *277* (20), 18021–18028.

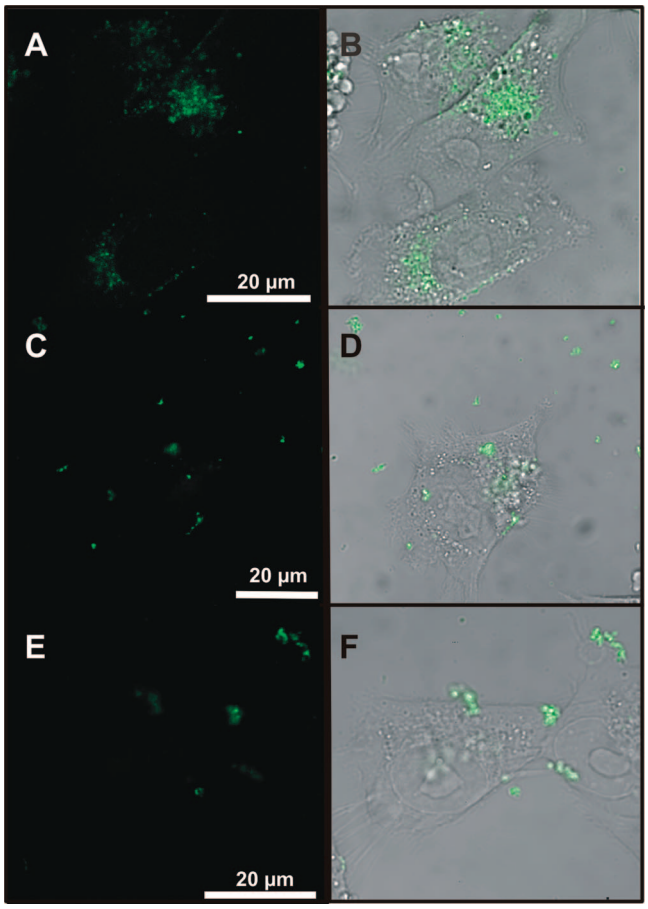

Figure 5. Effect of increasing MβCD concentrations on the uptake of non-PEGylated lipoplexes. Panels A, C and E are confocal fluorescence microscopy images, and B, D and F are overlays of the confocal images with the corresponding transmission images. (A, B) Uptake of non-PEGylated lipoplexes in the absence of MβCD. (C, D) Uptake of non-PEGylated lipoplexes in the presence of 500 μM MβCD. (E, F) Uptake of non-PEGylated lipoplexes in the presence of 1000 μM MβCD. Cells were preincubated with the inhibitor 2 h before addition of the non-PEGylated lipoplexes.

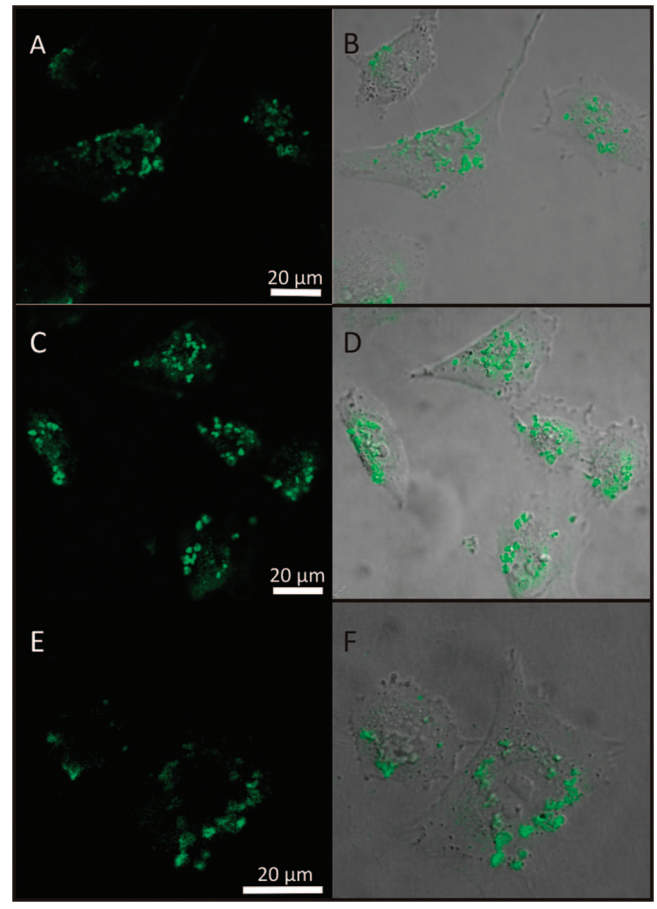

Figure 6. Effect of increasing MβCD concentrations on the uptake of PEGylated lipoplexes (originating from lipoplex loaded microbubbles exposed to ultrasound). Panels A, C and E are confocal fluorescence microscopy images, and B, D and F are overlays of the confocal images with the corresponding transmission images. (A, B) Uptake of PEGylated lipoplexes in the absence of MβCD. (C, D) Uptake of PEGylated lipoplexes in the presence of 500 μM MβCD. (E, F) Uptake of PEGylated lipoplexes in the presence of 1000 μM MβCD. Cells were preincubated with the inhibitor two hours before treatment with lipoplex loaded microbubbles and ultrasound.

In contrast to the free lipoplexes, the transfection efficiency of the PEGylated lipoplexes loaded on the microbubbles and exposed to ultrasound was by far less sensitive to MβCD treatment, as depicted in Figure 4 (dark gray bars). The lowest concentrations (100 to 500 μM) did not affect the transfection values at all. However, the transfection efficiency slightly dropped starting from 800 μM MβCD onward. We previously found that the ultrasound conditions used in these experiments had only a minor effect on the cell viability (results not shown). However, it might be possible that an extensive depletion of cholesterol may make cells more vulnerable to ultrasound. This may explain the drop in gene expression at higher MβCD concentrations (Figure 4, dark gray bars). Alternatively, depletion of cholesterol may change the fluidity of the plasma membrane.[37] As a result this may hamper the capability of ultrasound to cause cell perforations. Indeed, Brayman et al. suggested that the cell fluidity may influence the extent of membrane poration.[37] Finally, we also evaluated the effect of MβCD on the cellular uptake of lipoplex loaded microbubbles after exposure to ultrasound (Figure 6): images A and B, C and D, and E and F present the uptake of the lipoplexes in the presence of 0, 500, and 1000 μM MβCD, respectively. In contrast to the free lipoplexes, MβCD was not able to prevent the cellular uptake of lipoplexes that were released from the lipoplex loaded microbubbles after exposure to ultrasound. These results clearly prove that the PEGylated lipoplexes released from the microbubbles do not enter the cell by endocytosis after ultrasound radiation, this in contrast to the free lipoplexes.

(37) Brayman, A. A.; Coppage, M. L.; Vaidya, S.; Miller, M. W. Transient poration and cell surface receptor removal from human lymphocytes in vitro by 1 MHZ ultrasound. *Ultrasound Med. Biol.* **1999**, *25* (6), 999–1008.

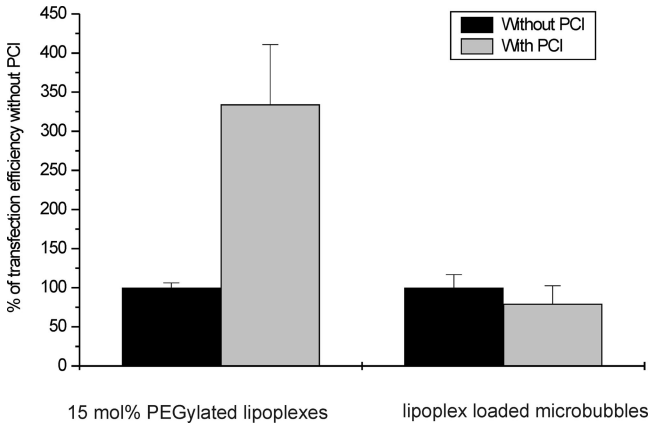

Figure 7. Effect of photochemical internalization (PCI) on the transfection efficiency of respectively 15 mol % PEGylated lipoplexes and lipoplex loaded microbubbles in the presence of ultrasound.

(b) Influence of Photochemical Internalization (PCI) on the Transfection Efficiency of Free PEGylated Lipoplexes and Lipoplex Loaded Microbubbles Exposed to Ultrasound. We evaluated the effect of PCI on the transfection efficiency of free 15 mol % PEGylated lipoplexes (which are poorly transfecting) and lipoplex loaded microbubbles in the presence of ultrasound. PCI was first presented in 1999 as a novel technology for the delivery of a variety of therapeutic molecules into the cytosol.[38] PCI technology employs amphiphilic, photosensitizing compounds which accumulate in the membranes of the vesicles. Upon illumination, such photosensitizers (PS) become excited, and subsequently induce the formation of reactive oxygen species, primarily singlet oxygens. These highly reactive intermediates can damage cellular components, but the short lifetime and, thus, the short range of action confine the damaging effect to the production site. This localized effect induces the disruption of the vesicles, thereby releasing the entrapped therapeutic molecules into the cytosol.[39]

Figure 7 demonstrates that the transfection efficiency of free 15 mol % PEGylated lipoplexes became three times higher when PCI was used. In contrast, the transfection efficiency of the lipoplex loaded microbubbles was not enhanced by PCI. Figure 7 proves that the endosomal release is indeed a barrier, though not the only one, in the gene transfection process with highly PEGylated lipoplexes. The fact that the gene transfer by the same lipoplexes but loaded onto microbubbles and treated with ultrasound was not altered upon PCI implies that the lipoplexes released from the microbubbles are not present in the endosomes. These observations suggest that they transfect cells through a nonendocytic uptake mechanism that delivers the lipoplexes directly in the cytoplasm of the cells.

(c) What Happens at the Cellular Membrane during Exposure of Lipoplex Loaded Microbubbles to Ultrasound? First we studied the uptake of green labeled 15 mol % PEGylated lipoplexes into BLM-cells (at 37 °C) by confocal microscopy (Figure 8). Figure 8A presents the cellular uptake of free lipoplexes 30 min after addition to the cells, while Figure 8B and Figure 8C present the cellular uptake of the same lipoplexes 150 min after addition to the cells. Free lipoplexes started to stick on the cell membranes shortly after their addition to the cells (Figure 8A). As indicated in Figure 8A, lipoplexes were not internalized 30 min after addition to the cells. Only after 150 min the lipoplexes were internalized by the BLM-cells: a punctuate pattern was observed which indeed suggests an endocytic uptake for the free PEGylated lipoplexes (Figure 8B,C). In contrast, we saw a completely different pattern 30 min after sonication of the cells in the presence of the lipoplex loaded microbubbles (Figure 8D). Lipoplexes were present near the cellular membrane and inside the cell. Similar images were obtained 150 min after treatment of the cells with lipoplex loaded microbubbles and ultrasound (Figure 8E,F); these images indicate that the uptake of the lipoplexes released from the microbubbles occurs during or immediately after ultrasound treatment.

To get further insights into the effect on the cell membrane we stained the cell membrane and took z-stacks of the BLM cells after incubating them with respectively free PEGylated lipoplexes (Figure 9A,C) and lipoplex loaded microbubbles exposed to ultrasound (Figure 9B,D). The first important difference between the images in Figure 9A and Figure 9B is the irregular shape of the BLM cells after sonication. This was also observed by several other groups.[18,37,40−42] Although the shape of the cells was different after exposure to ultrasound and microbubbles, our propidium iodide uptake experiments proved that the cells were still viable (see Figure 10). In the image in Figure 9A, a smooth, undisturbed cell membrane is visible (red) with PEGylated lipoplexes (green) lying on top of it, while a small part of the lipoplexes seems present in endocytic vesicles. Figure 9C displays the intensity profile of the green and red fluorescence following an *X*-axis (being the dotted line in Figure 9A) through the cell. This

(38) Berg, K.; Selbo, P. K.; Prasmickaite, L.; Tjelle, T. E.; Sandvig, K.; Moan, J.; Gaudernack, G.; Fodstad, O.; Kjolsrud, S.; Anholt, H.; Rodal, G. H.; Rodal, S. K.; Hogset, A. Photochemical internalization: a novel technology for delivery of macromolecules into cytosol. *Cancer Res.* **1999**, *59* (6), 1180–1183.

(39) Prasmickaite, L.; Hogset, A.; Tjelle, T. E.; Olsen, V. M.; Berg, K. Role of endosomes in gene transfection mediated by photochemical internalisation (PCI). *J. Gene Med.* **2000**, *2* (6), 477–488.

(40) Ross, J. P.; Cai, X.; Chiu, J. F.; Yang, J.; Wu, J. R. Optical and atomic force microscopic studies on sonoporation. *J. Acoust. Soc. Am.* **2002**, *111* (3), 1161–1164.

(41) Schlicher, R. K.; Radhakrishna, H.; Tolentino, T. P.; Apkarian, R. P.; Zarnitsyn, V.; Prausnitz, M. R. Mechanism of intracellular delivery by acoustic cavitation. *Ultrasound Med. Biol.* **2006**, *32* (6), 915–924.

(42) Zhao, Y. Z.; Luo, Y K.; Lu, C. T.; Xu, J. F.; Tang, J.; Zhang, M.; Zhang, Y.; Liang, H. D. Phospholipids-based microbubbles sonoporation pore size and reseal of cell membrane cultured in vitro. *J. Drug Targeting* **2008**, *16* (1), 18–25.

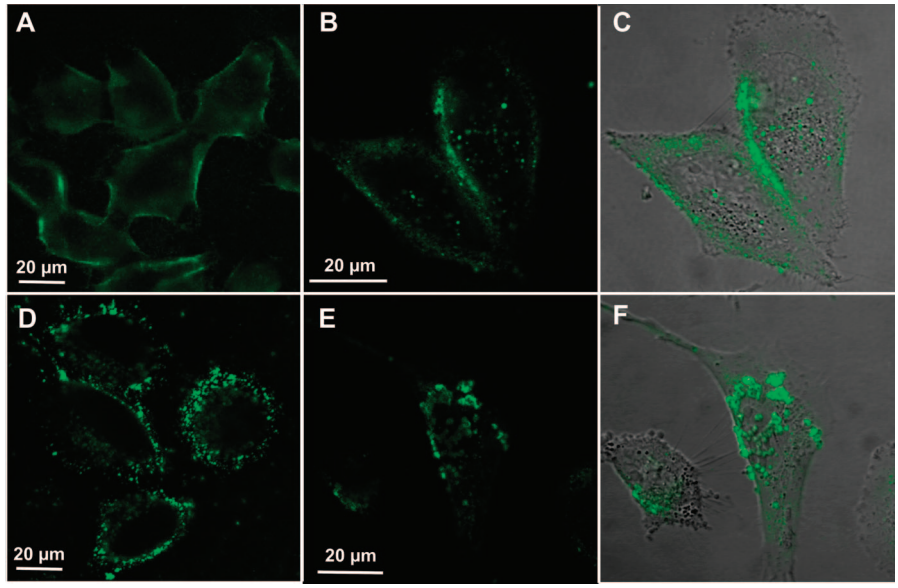

Figure 8. (A) Uptake of free 15 mol % PEGylated lipoplexes in BLM cells at 30 min incubation after addition to the cells. (B, C) Uptake of free 15 mol % PEGylated lipoplexes in BLM cells after 150 min incubation time. (D) Uptake of lipoplexes in BLM cells 30 min after treatment with lipoplex loaded microbubbles and ultrasound. (E, F) Uptake of lipoplexes in BLM cells 30 min after treatment with lipoplex loaded microbubbles and ultrasound. Lipoplexes were labeled with Bodipy FlC12 cholesteryl. Panels A, B, C and D are confocal fluorescence microscopy images, and panels C and F are the overlays of the confocal images B and E with the corresponding transmission image.

intensity profile in Figure 9C confirms that the lipoplexes are attached to the cell membrane as the green fluorescence of the lipoplexes colocalizes with the red fluorescence of the cell membrane. In Figure 9B the PEGylated lipoplexes appear as bright green structures pinching through the cell membrane. Furthermore the cell membrane seems disturbed and lipids seems to be relocated, resulting in lipid enhanced areas and areas lacking cell membrane lipids. Lipoplexes and membrane lipids seemed partially colocalized, visible as the yellow parts. Earlier, Schlicher et al. also reported on the displacement of large lipid areas from the cell membrane upon ultrasound treatment.[41] Also the intensity profile (Figure 9D) of this cell looks completely different: green lipoplexes are visible within the cell borders and the red colored cell membranes are partially displaced into the cytoplasm.

The green spot in Figures 8E and 9B most likely originates from intact lipolexes as we recently showed that intact lipoplexes are released from the microbubbles after sonication of the lipoplex loaded microbubbles.[22] To be effective these lipoplexes must dissociate intracellularly, so that the DNA can enter the cell nucleus for transcription. Zuhorn and colleagues demonstrated that, after endosome rupture by osmotic shock, lipoplexes still showed the same transfection efficiency, indicating that intact lipoplexes can dissociate in the cytosol.[43] This is most likely also the case for the lipoplexes present in the BLM cells after their release from the lipoplex loaded microbubbles, as they have a very high transfection efficiency.

(d) Why Is the Coupling of the Lipoplexes to the Microbubbles So Important? Figure 2B shows that the transfection efficiency of free PEGylated lipoplexes does not improve upon (physically) mixing them with microbubbles and applying ultrasound (dark gray bars). Therefore, we wondered whether the cells were perforated under our ultrasound conditions. To demonstrate the presence of pores in the cell membrane we determined whether propidium iodide (PI) was able to enter the cells during ultrasound exposure. Figure 10A presents the uptake of PI during incubation of the BLM cells with lipoplexes: as expected, none of the BLM cells was able to take up PI. Figure 10B is an image of BLM cells to which PI, PEGylated lipoplexes and microbubbles were added and which were exposed to ultrasound. Almost all the cells had a bright red fluorescent nucleus, due to PI, which indicates that upon sonication pores are indeed created in the cell membranes which allow the passage of small molecules like PI.[18,30,33] To exclude the possibility that all the red colored cells were dead cells, we added PI 15 min after the exposure of the cells to ultrasound as only dead cells would then be able to take up PI; living cells are expected to quickly reseal their (transient) pores after applying ultrasound. As demonstrated in Figure 10C, only a small fraction of the cells took up PI, which proves that the uptake of PI in Figure 10B can be ascribed to short-living pores in the cell membrane caused by ultrasound in the presence of microbubbles.

Our data show that the attachment of the PEGylated lipoplexes to microbubbles is required to obtain a good gene transfer in the presence of ultrasound. We would like to

(43) Zuhorn, I. S.; Visser, W. H.; Bakowsky, U.; Engberts, J. B. F. N.; Hoekstra, D. Interference of serum with lipoplex-cell interaction: modulation of intracellular processing. *Biochim. Biophys. Acta* **2002**, *1560* (1−2), 25–36.

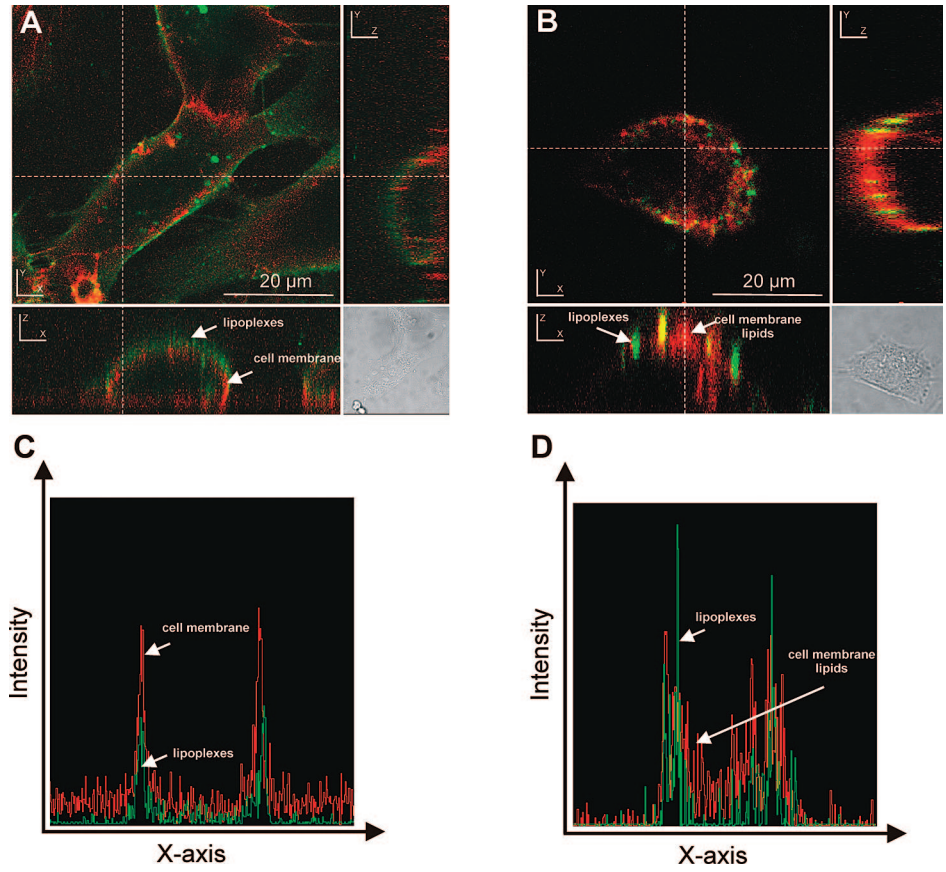

Figure 9. Panel A displays a confocal fluorescence microscopy image and z-scans (at the position indicated by the white dotted line) of a BLM cell that was incubated during 30 min with free PEGylated lipoplexes. Panel B displays a confocal fluorescence microscopy image and z-stacks, at the position indicated by the white dotted line, of BLM cells 30 min after treatment with lipoplex loaded microbubbles and ultrasound. The cell membrane was labeled red with concanavalin A-Alexa647, and PEGylated lipoplexes are visible in green. Panels C and D present the according intensity profiles of respectively image A and image B following the *X*-axis (white dotted line) through the cell.

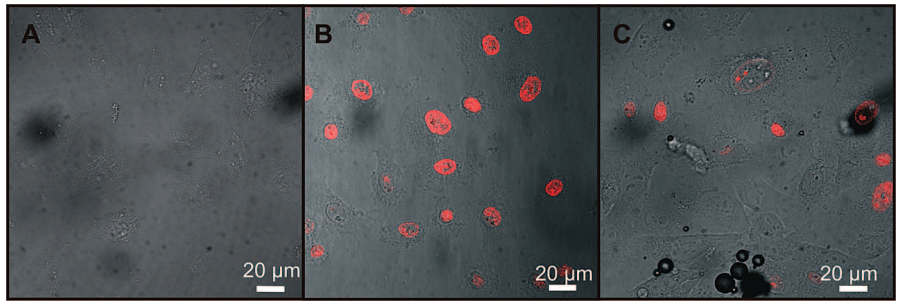

Figure 10. Cellular uptake of propidium iodide (PI) in BLM cells. (A) PI uptake during incubation of the cells with free PEGylated lipoplexes. (B) PI uptake in cells simultaneously exposed to PI, free PEGylated lipoplexes, microbubbles and ultrasound. (C) Confocal image of cells that were first treated with free PEGylated lipoplexes, microbubbles and ultrasound and subsequently, after 15 min, exposed to PI.

present two hypotheses that may explain why the lipoplexes should be attached to the microbubbles. First, as the microbubbles rise against the cell surface, it is possible that the massive release of lipoplexes upon ultrasound radiation results in a higher lipoplex concentration near the cell perforations, which might increase the amount of lipoplexes that is able to passively diffuse through these pores. We estimated the concentration of lipoplexes released near the cells after exposure of the lipoplex loaded microbubbles to ultrasound. Therefore, we first determined how much of the lipoplexes is bound to the microbubbles after mixing the biotinylated lipoplexes and avidinylated microbubbles. Half of the lipoplexes is able to bind to the microbubbles (data not shown). As presented in Figure 1B, the Opticells were incubated with the cell monolayer on top, so that microbubbles could rise against the cell surface. Let us assume that, after exposure of the lipoplex loaded microbubbles to ultrasound, all the lipoplexes are released in a 20 μm thick

plane just beneath the cells present on the Opticell unit. The volume then equals 100 μL (an Opticell unit has a surface of 50 cm^2). Taking into account that half of the lipoplexes are attached to the microbubbles, we can calculate that the local concentration of lipoplexes near the cell membrane (i.e., the concentration near the cell perforations) is 50 times higher than the lipoplex concentration near the cells when uncoupled lipoplexes are mixed with microbubbles and exposed to ultrasound. Thus, the first hypothesis makes sense if the lipoplexes are small enough to pass through the cell perforations. This might be the case as pores of up to 1 μm have been reported.[41] However, one should realize that this pore size cannot be extrapolated to our work as the size of the cell perforations most likely depends on ultrasound conditions and cell type used.

The second hypothesis is that the microjets that occur when the microbubbles collapse drag along the released lipoplexes and inject them in and through the cell membrane. Ohl et al. and Dijkink et al. previously described the appearance of a jetting flow after the collapse of microbubbles in an ultrasonic field.[44,10] This flow is directed toward the cell layer and causes shear stress on the cells which results in pore formation. During the implosion of the microbubbles, the lipoplexes are released and can be taken by this jetting flow toward the cell surface. In this way it might be possible that lipoplexes become injected into the cell layer when the streaming forces are high enough. Our data obtained via confocal microscopy support this hypothesis (Figure 9). Additionally, Marmottant and Hilgenfeldt[45] visualized the behavior of a lipid vesicle in the presence of a stable cavitating microbubble. This vesicle was expelled away from the cavitating microbubbles. It is possible that lipoplexes are taken by these fluid streams around the microbubble and in this way propelled, so that they are deposited in the adjacent cell layer. Especially as most of our microbubbles are cavitating transiently and are able to implode, even stronger streaming forces will occur. The actual lipoplex uptake will most presumably be a combination of the two described hypotheses, as an increased local lipoplex concentration will make it more plausible that a lipoplex is taken by these fluid streams and increases the chance that it is deposited near or in the cell membrane (pores).

As earlier mentioned, the aim of this work was to elucidate how the transfection efficiency of PEGylated lipoplexes can be increased by loading them onto lipid microbubbles and exposing them to ultrasound. Our results clearly show that endocytosis of the lipoplexes is circumvented and that lipoplexes are able to reach the cytoplasm of the radiated cells. However, direct microscopic observations of the lipoplex loaded microbubbles during ultrasound exposure are required to elucidate the exact uptake mechanisms.

Conclusion

In this study we elucidate the cellular mechanism responsible for the high gene transfection efficiency of lipoplex loaded microbubbles in the presence of ultrasound. Inhibition of the endocytotic activity of the cells demonstrated that the cellular uptake of the lipoplexes released from the lipoplex loaded microbubbles by ultrasound must be governed by a nonendocytotic pathway. Indeed, blockage of the endocytotic activity or stimulation of the endosomal release via PCI did not affect the gene expression of the lipoplex loaded microbubbles after exposure to ultrasound. Confocal images demonstrated that, shortly after exposure of the BLM cells to lipoplex loaded microbubbles and ultrasound, lipoplexes are present in the cell membrane and in the intracellular space. In contrast, classic "free" PEGylated lipoplexes mainly adhere on top of the cell membranes. We also observed that the cell membranes became disturbed after applying ultrasound and lipoplex loaded microbubbles. The addition of propidium iodide during the sonication step proved that there were short-living pores formed. As ultrasound could not improve the gene transfer of PEGylated lipoplexes that were physically mixed (and thus not chemically bound) to microbubbles, it seems that coupling of lipoplexes and microbubbles is necessary to obtain a high transfection value. Loading of the lipoplexes onto the microbubbles leads to an increase in local lipoplex concentration near the cell membrane. Because we have shown that cell membrane porations are formed during our ultrasound exposure, it is possible that more lipoplexes are able to passively diffuse through these pores. Moreover, lipoplexes might be propelled by the fluid streams that develop around a cavitating and imploding microbubble and propelled inside the adjacent cell layer. However, real time fluorescence imaging of the lipoplexes during the ultrasound step will be required to completely understand their cellular entrance. In summary, we have proven that the endocytotic uptake of PEGylated particles can be avoided by loading these particles onto microbubbles and applying ultrasound. In this manner the lipoplexes become directly delivered into the cytoplasm of the cell. So far the lack of gene transfer hampered the clinical use of PEGylated lipoplexes. We believe that lipoplex loaded microbubbles may overcome this. Clearly, besides lipoplexes one can also attach other drugs or drug containing nanoparticles to the microbubbles, which makes this material of special interest for time and space controlled delivery of drugs.

Acknowledgment. I.L. is a doctoral fellow of Fund for Scientific Research-Flanders. N.N.S. is a Postdoctoral Fellow of the Fund for Scientific Research-Flanders (Belgium). The financial support of FWO, BOF-Ghent and the European Union (via the FP7 Projects Arise and SonoDrugs) is acknowledged.

MP800154S

(44) Dijkink, R.; Le, G. S.; Nijhuis, E.; van den, B. A.; Vermes, I.; Poot, A.; Ohl, C. D. Controlled cavitation-cell interaction: transmembrane transport and viability studies. *Phys. Med. Biol.* **2008**, *53* (2), 375–390.

(45) Marmottant, P.; Hilgenfeldt, S. Controlled vesicle deformation and lysis by single oscillating bubbles. *Nature* **2003**, *423* (6936), 153–156.